

Mechanistic Modeling of Tumor Repopulation during Radiation Treatments

Antonio Mario Locci*

Dipartimento di Ingegneria Meccanica, Chimica e dei Materiali, Università degli Studi di Cagliari, Via Marengo 2, Cagliari, 09123 Italy

Abstract

A mechanistic mathematical model for radiotherapy is developed to study the effect of tumor repopulation on radiation treatment outcome. The Two-Lesion Kinetic (TLK) model is adopted to describe the interaction between ionizing radiation and malignant cells, and extended in this work to take into account tumor proliferation. The investigated kinetics for tumor cells growth includes exponential, logistic and Gompertz laws, while standard fractionation treatments are considered as case studies. Scaling analysis is used for non-dimensionalizing the system of ordinary differential equations describing the process under investigation. Numerical solution of the proposed model is shown as a function of the dimensionless variables and groups generated by the scaling procedure. The latter allows minimizing the number of parameters needed to describe the radiotherapy process when DNA damage formation and repair, and tumor repopulation phenomena take place simultaneously.

The effectiveness in tumor eradication is mapped as a function of two dimensionless groups that take into account the radiation dose rate as well as the DNA lesions repair and malignant cells repopulation rates. The present study illustrates that outcomes of the radiotherapy treatment are strongly affected by the relative rates of phenomena simultaneously occurring. In particular, it appears that in order to achieve an effective treatment by keeping as low as possible the total dose to be administered, the fractionation scheme should be optimized on the base of the ratio between the DNA repair mechanisms and tumor cell growth rates. Model results also show that exponential and logistic kinetics yield similar results in terms of treatments outcomes. By comparison, model simulations with the Gompertz law indicate that repopulation described by this growth kinetics result in a significantly poorer prognosis for tumor eradication than either exponential or logistic models.

Keywords: Modeling; Kinetics; Radiotherapy; Repopulation; DNA lesions repair

Introduction

Radiotherapy is a common treatment for cancer, which aim is to destroy malignant cells with radiation while limiting the damage to nearby normal (healthy) cells [1]. If tumor cells respond to irradiation at lower doses than normal tissue, then a therapeutic window exists, in which a variety of treatment protocols can be used to eradicate the tumor while sparing healthy tissues. However, a therapeutic window may be nonexistent if tumor and normal tissues respond similarly to irradiation [2]. Despite the steady increase in our molecular knowledge of tumor cells, most treatment strategies, including radiotherapy, do not affect cancer cells uniquely but all proliferating cells. Radiotherapy is typically successful because host cells are for the most part non-proliferative and have better repair mechanisms than tumor cells [1].

The time course of radiation dose delivery affects the results in many ways. For example, given the total prescribed dose, prolonging treatment over a number of weeks allows time for repair of radiation damage to surrounding normal tissue [3]. It may also favor tumor re-sensitization because cellular radiosensitivity is enhanced by time-dependent processes such as cell cycle progression or tumor reoxygenation [4]. Furthermore, one should keep the overall time as short as possible to avoid excessive tumor proliferation, and many clinical results already underscore the importance of this factor [5].

Any attempt to determine desirable dose timing needs then to balance several factors, which often oppose each other [6]. The only tool potentially capable of handling the entire picture is mathematical modeling. It can play a crucial role in developing the tumor radiological cure by giving vital insights into whether a particular treatment schedule may be suitable or not to be used in a clinical setting [6]. The results of such modeling can also potentially inform the radiation oncologist on how to tailor treatment plans for individual patients. Mathematical models, also known as *in silico* models, can be further

utilized to predict the success or failure of virtual and novel treatment protocols [7,8].

Mathematical modeling of radiotherapy comes in various degrees of complexity depending on the well-established five "R's" of radiobiology that are incorporated into the models, i.e., the four "R's" by Withers, i.e., Repair, Repopulation, Redistribution and Reoxygenation [9] and more recently Resensitization [10]. However, of the five R's of radiotherapy that exist, it has emerged from clinical studies that repopulation is one of the most significant factors that can provide insight into the lack of efficacy of radiation treatment [11]. This is because radiotherapy treatment schedules are fractionated to allow normal tissue to repair and recover from irradiation. During these periods of recovery and rest, surviving clonogenic cells of the tumor also repair and repopulate, which may result in the failure of the treatment. Indeed, the nature of the re-growth of particular tumor concerned is expected to influence the outcome of a specific treatment schedule [12,13]. As an example, optimum fractionation schedules for treatment of head and neck cancer or non-small cell lung cancer depend critically on the proliferative nature of the tumor cells [11]. In these cases, tumors proliferate so fast that shorter schedules are required [14].

Clearly, mathematical modeling of radiotherapy treatments will be more accurate if repopulation effects are included based on

*Corresponding author: Antonio Mario Locci, Dipartimento di Ingegneria Meccanica, Chimica e dei Materiali, Università degli Studi di Cagliari, Via Marengo 2, Cagliari, 09123 Italy, Tel: 39 070 675 5077; E-mail: antonio.locci@dimcm.unica.it

Received May 11, 2015; Accepted May 20, 2015; Published May 30, 2015

Citation: Locci AM (2015) Mechanistic Modeling of Tumor Repopulation during Radiation Treatments. J Chem Eng Process Technol 6: 226. doi:10.4172/2157-7048.1000226

Copyright: © 2015 Locci AM. This is an open-access article distributed under the terms of the Creative Commons Attribution License, which permits unrestricted use, distribution, and reproduction in any medium, provided the original author and source are credited.

the biological proliferation rate of the tumor. As a consequence, mathematical models including this aspect may be clinically useful in predicting response to therapy [15]. This may also lead to a better understanding of clinical implications of the different re-growth laws that may be acting during the course of radiation treatments of cancer and therefore repopulation should be considered during their planning [11].

The debate on the importance of repopulation effects has led to several models with specific growth laws being proposed to describe tumor proliferation and re-growth [16-25]. The purpose of this article is then to provide a contribution in radiobiological modeling applied to external beam radiotherapy. In particular, the Two-Lesion Kinetic (TLK) model for describing radiation cell killing is adopted [26]. In this work, the TLK model is extended for the first time, at the best of author's knowledge, to include the role of cellular repopulation during radiotherapy treatments. In addition, a minimum parametric representation of this process is obtained by applying a scaling analysis [27]. This approach allows mapping out the relevant scenarios that can occur during radiotherapy when radiation damages formation and repair, and tumor repopulation phenomena take place simultaneously.

Mathematical Model

Let N denote the number of clonogenic tumor cells of the population to be studied. The following ordinary differential equation can be written to describe its dynamics:

$$\frac{dN}{dt} = B(N,t) - H(N,t) \quad (1)$$

along with the initial condition

$$N = N_0 \text{ @ } t = 0 \quad (2)$$

The functions B and H represent the birth rate of the cells population and its radiation-induced death rate, respectively. It is worth mentioning that the natural cell death rate was neglected in this work. The reader should refer to the nomenclature section for significance of symbols appearing in the text.

The birth rate represents the tumor cells growth, which has been mathematically described in the literature by several expressions. In particular, it has been reported that exponential growth provides a very good approximation to the kinetics of early stage tumor growth, but loses accuracy at larger tumor sizes. Indeed, it has been found that the tumor growth rate will be slowed as the tumor reaches a larger size, being in this case better modeled by a logistic or Gompertz law [28]. With the aim not to limit the investigation to a specific kinetics, in this work tumor growth in terms of cell population has been modeled by using all the following kinetics:

$$B = k_B N \quad (3)$$

$$B = k_B N \left(1 - \frac{N}{K} \right) \quad (4)$$

$$B = k_B N \ln \left(\frac{K}{N} \right) \quad (5)$$

which express the exponential, logistic and Gompertz law, respectively [29].

The radiation-induced death rate appearing in Equation 1 embodies the effects of radiotherapy on tumor cells population. Explicitly, the function H can be defined as

$$H(t) = h(t)N(t) \quad (6)$$

where the hazard function h can be expressed in terms of the well-known survival probability, S , i.e., the expected fraction of the cells capable of producing viable progeny after irradiation [6]

$$h(t) = \frac{1}{S(t)} \frac{dS}{dt} \quad (7)$$

With the aim to express the survival probability S at time t , the mechanisms underlying the interaction between cells and radiation should be taken into account. When ionizing radiation strikes a cell, Double Strand Breaks (DSBs) and other lesions are produced in DNA within a characteristic time less than a millisecond [30]. Thereafter some of the damages are processed more slowly, in enzymatic repair or misrepair reactions, whose outcome determines the fate of the cell.

In this work, the Two-Lesion Kinetic (TLK) model, which was proposed to make a better link between biochemical processing of DSBs and cell killing, is adopted [26]. A defining feature of the TLK model is that the family of all possible DSBs is subdivided into simple and complex DSBs, and each kind of DSB may have its own unique repair characteristics. Simple DSBs (type 1) are assumed to be a section of the DNA 10 to 20 base pairs in length that contains a break in both strands of the DNA. On the other hand, a complex DSB (type 2) is a simple DSB that contains additional elementary damage sites (base damage, strand breaks, base deletion, etc.) within the same section of DNA. Break-ends associated with both kinds of DSB are also allowed to interact in pairwise fashion to form irreversible lethal and non-lethal chromosome aberrations.

Taking advantage of this description, a mechanistic model based on a system of ordinary differential equations to link formation and repair of DSBs induced by radiation to cell killing was developed [26]. The most general form of the TLK model uses 16 biologically significant parameters to relate biochemical processing of the DSB to mutagenesis and cell killing. However, in this work it has been used a variant of the TLK model that retains most of the central features of the full model, while reducing the number of parameters from 16 to 10 [31]. More specifically, the following pair of nonlinear differential equations models the time-dependent evolution of the DSBs created and then repaired, misrepaired or fixed:

$$\frac{d\bar{L}_1}{dt} = 2\dot{D}Y\Sigma_1 - \lambda_1\bar{L}_1 - \eta\bar{L}_1(\bar{L}_1 + \bar{L}_2) \quad (8)$$

$$\frac{d\bar{L}_2}{dt} = 2\dot{D}Y\Sigma_2 - \lambda_2\bar{L}_2 - \eta\bar{L}_2(\bar{L}_1 + \bar{L}_2) \quad (9)$$

where \dot{D} is the instantaneous absorbed dose rate, \bar{L}_1 is the expected number of simple (type 1) DSBs per cell and \bar{L}_2 is the expected number of complex (type 2) DSBs per cell. The initial DSB yield Y represents the number of bps per cell (the factor of 2 converts bp to number of nucleotides), and Σ_i are the DSBs formation probabilities. The parameter λ_i characterizes the rate at which lesions (DSBs) are removed by rejoining the break-ends formed in DNA molecules. This is attained through biochemical enzymatic processes that repair individual simple or complex lesions. DNA damages may be also removed through a pairwise (quadratic or binary misrepair) damage interaction process whose rate is expressed by η . Thus, both λ_i and η can be related to the expected amount of time required for a cell to remove DSBs generated by radiation through the corresponding repair mechanisms. The biophysical interpretation of these parameters is discussed in more detail elsewhere [26].

The number of lethal lesions or genetic alterations is modelled by the following equation [31]

$$\frac{d\bar{L}_f}{dt} = (1 - a_1)\varphi_1\lambda_1\bar{L}_1(t) + (1 - a_2)\varphi_2\lambda_2\bar{L}_2(t) + \gamma\eta[\bar{L}_1(t) + \bar{L}_2(t)]^2 \quad (10)$$

where a_1 and a_2 represent the fidelity of the linear misrepair mechanisms for type 1 and type 2 DSB, respectively, (e.g., $a_i=1$ indicates correct repair). The probabilities φ_i and γ partition misrepaired damages into lethal and non-lethal genetic alterations (e.g., $\varphi_i=1$ means that linear misrepair of a DSB always produces a fatal lesion).

Once the number of lethal lesions or genetic alterations (point mutations or chromosome aberrations) per cell \bar{L}_f is obtained, the survival probability can be expressed as follows [26]:

$$S(t) = \exp(-\bar{L}_f) \quad (11)$$

and by combining Eqs. (6), (7) and (11) it can be obtained that

$$H(t) = N(t) \frac{d\bar{L}_f}{dt} \quad (12)$$

Although the TLK model may suffice to link biochemical processing of the DSB to cell killing, the number of parameters used in this model can be prohibitive for some applications, if the parameters are treated as purely *ad hoc* [31]. Through the use of biologically meaningful equality and inequality constraints, the number of free parameters used in the TLK can be effectively reduced to a level comparable to the classical LQ or other models. In particular, the standard, three-parameter LQ model can be mimicked using the TLK formalism by imposing the equality constraints: $a_1 = a_2$, $\varphi_1 = \varphi_2$, $\lambda_1 = \lambda_2$, and $\Sigma_1 = \Sigma_2$ [31].

By using these simplifications, Equations 8-9 are summed up to obtain the following equation

$$\frac{d\bar{L}}{dt} = 4\dot{D}Y\Sigma - \lambda\bar{L} - \eta\bar{L}^2 \quad (13)$$

where \bar{L} represents the total number of DSBs expected per cell. Equation 10 can be also rewritten as

$$\frac{d\bar{L}_f}{dt} = (1 - a)\varphi\lambda\bar{L} + \gamma\eta\bar{L}^2 \quad (14)$$

Substituting Equation 14 into Equation 12 the balance equation for the number of clonogenic tumor cells can be expressed as

$$\frac{dN}{dt} = B - N \left[(1 - a)\varphi\lambda\bar{L} + \gamma\eta\bar{L}^2 \right] \quad (15)$$

The system of non-linear ordinary differential equations 13 and 15 completely described the radiotherapy treatment when repopulation occurs simultaneously to cell killing induced by radiation. However, this mathematical model depends on 8 parameters. In order to obtain a minimum parametric representation of this process, a scaling analysis is applied in this work [27]. Briefly, scaling analysis deals with a systematic method for non-dimensionalizing a system of describing equations of the process under investigation. By the resulting dimensionless system of equations it means that the solution for any quantity that can be obtained from these equations will be at most a function of the dimensionless independent variables and the dimensionless groups generated by the scaling process. This minimum parametric representation of the process is useful since it identifies the dimensionless variables and groups that can be used to correlate data from laboratory or numerical experiments (i.e., computer simulations). Moreover, it can be assessed the relative importance of the various

phenomena taking place during the investigated process.

The scaling analysis procedure for the system under investigation is illustrated in the next. Let us define the following dimensionless variables

$$\Lambda = \frac{\bar{L} - \bar{L}_r}{\bar{L}_s} \quad (16)$$

$$N = \frac{N - N_r}{N_s} \quad (17)$$

$$\tau = \frac{t}{t_s} \quad (18)$$

where the subscripts r and s represent the reference and the scaling values of corresponding variables [27]. Hereafter, upper- or lower-case Greek letters will indicate dimensionless variables or groups of them. By setting $\bar{L}_r = N_r = 0$, $N_s = N_0$,

$$\bar{L}_s = \frac{1}{(1 - a)\varphi} \quad (19)$$

and

$$t_s = \frac{1}{k_B} \quad (20)$$

the following dimensionless governing equations can be derived

$$\frac{dN}{d\tau} = N\Phi(N) - N\Lambda \left(\Lambda + \Delta X \Lambda^2 \right) \quad (21)$$

$$\frac{d\Lambda}{d\tau} = \Lambda - B\Lambda - X\Lambda^2 \quad (22)$$

It should be point out that Equation 20 implies that the characteristic time of cell growth is adopted as time scale of the process under investigation. This choice stems out being the aim of this work to analyze the effect of tumor repopulation during radiation treatment.

The function $\Phi(N)$ appearing in Equation 21 represents the dimensionless form of the tumor cells growth kinetics. Specifically,

$$\Phi = \begin{cases} 1 \\ 1 - \frac{N}{E} \\ \ln\left(\frac{E}{N}\right) \end{cases} \quad (23)$$

depending on the exponential, logistic, or Gompertz growth kinetics, respectively, is adopted.

The dimensionless groups appearing in Equations 21 and 23 have the following expression

$$A = \frac{4\dot{D}Y\Sigma(1 - a)\varphi}{k_B} \quad (24)$$

$$B = \frac{\lambda}{k_B} \quad (25)$$

$$X = \frac{\eta}{(1-a)\phi\lambda} \quad (26)$$

$$\Delta = \frac{\gamma}{(1-a)\phi} \quad (27)$$

$$E = \frac{K}{N_0} \quad (28)$$

The parameter A can be interpreted as the ratio between the DSBs production rate and the tumor cell proliferation rate. Therefore, high values of A (say greater than one) mean that DNA lesions are produced faster than tumor cell increases in number. The opposite holds when A is smaller than one. On the base of its expression, A can be also identified as the dimensionless DSBs production rate. Similar considerations can be made on the parameter B. Indeed, it is the ratio between the rate at which damages are repaired by the linear mechanism and the tumor growth rate. Again, higher values of B imply that lesions are repaired faster than tumor cells repopulate. Moreover, B may be regarded as the dimensionless linear repair rate. Following the same line of reasoning, the dimensionless parameter X defined by Equation 26 represents the ratio between the rate of binary misrepair and linear repair mechanisms. This implies that high values of X correspond to a faster binary misrepair mechanism with respect to the linear one. Clearly, the opposite holds in the case of low X. The parameter Δ is the ratio between probabilities of binary and linear repair mechanisms to generate a lethal DNA lesion. Finally, the parameter E can be taken as the dimensionless carrying capacity.

The instantaneous dose rate \dot{D} appearing in Equation 13 is dependent on the total radiation dose D prescribed by clinical protocol and on the treatment schedule adopted. In particular, the following relationship holds

$$D(T) = \int_0^T \dot{D}(t) dt \quad (29)$$

being T the entire period of treatment. However, in tumor radiotherapy using external beams a wide variety of protocols is employed. Thus, in this work, a general expression of the dose rate \dot{D} is derived in order to increase the applicability of the proposed model.

The treatment time T can be divided into a number n of cycle consisting of an irradiation period (hereafter identified as t_{Session}) followed by a recovery time. The latter is a period during which radiation is not delivered and normal (healthy) tissues are allowed repairing radiation damages. It descends that the cycle time t_{Cycle} is given by

$$t_{\text{Cycle}} = \frac{T}{n} \quad (30)$$

Taking advantage of the parameters defining the irradiation schedule reported above, the dose rate may be expressed as follows:

$$\dot{D} = \begin{cases} \frac{D}{nt_{\text{Session}}} & \text{if } \text{int}\left(\frac{t}{t_{\text{Cycle}}}\right) \leq \left(\frac{t}{t_{\text{Cycle}}}\right) \leq \text{int}\left(\frac{t}{t_{\text{Cycle}}}\right) + \frac{t_{\text{Session}}}{t_{\text{Cycle}}} \\ 0 & \text{if } \left(\frac{t}{t_{\text{Cycle}}}\right) > \text{int}\left(\frac{t}{t_{\text{Cycle}}}\right) + \frac{t_{\text{Session}}}{t_{\text{Cycle}}} \text{ and } \left(\frac{t}{t_{\text{Cycle}}}\right) < \text{int}\left(\frac{t}{t_{\text{Cycle}}}\right) + 1 \end{cases} \quad (31)$$

where "int" indicates the function giving the integer part of a real

number as a result. It may be realized from Equation 31 that the same total dose and dose rate can be imposed to the system with different treatment schedule by appropriately varying the parameter n and t_{Session} .

A dimensionless version of Equation 31 can be now derived by using Equations 15 and 21. Specifically, it can be obtained that

$$A = \begin{cases} A^* & \text{if } \text{int}\left(\frac{\tau}{\tau_{\text{Cycle}}}\right) \leq \left(\frac{\tau}{\tau_{\text{Cycle}}}\right) \leq \text{int}\left(\frac{\tau}{\tau_{\text{Cycle}}}\right) + \frac{\tau_{\text{Session}}}{\tau_{\text{Cycle}}} \\ 0 & \text{if } \left(\frac{\tau}{\tau_{\text{Cycle}}}\right) > \text{int}\left(\frac{\tau}{\tau_{\text{Cycle}}}\right) + \frac{\tau_{\text{Session}}}{\tau_{\text{Cycle}}} \text{ and } \left(\frac{\tau}{\tau_{\text{Cycle}}}\right) < \text{int}\left(\frac{\tau}{\tau_{\text{Cycle}}}\right) + 1 \end{cases} \quad (32)$$

being A^* defined as

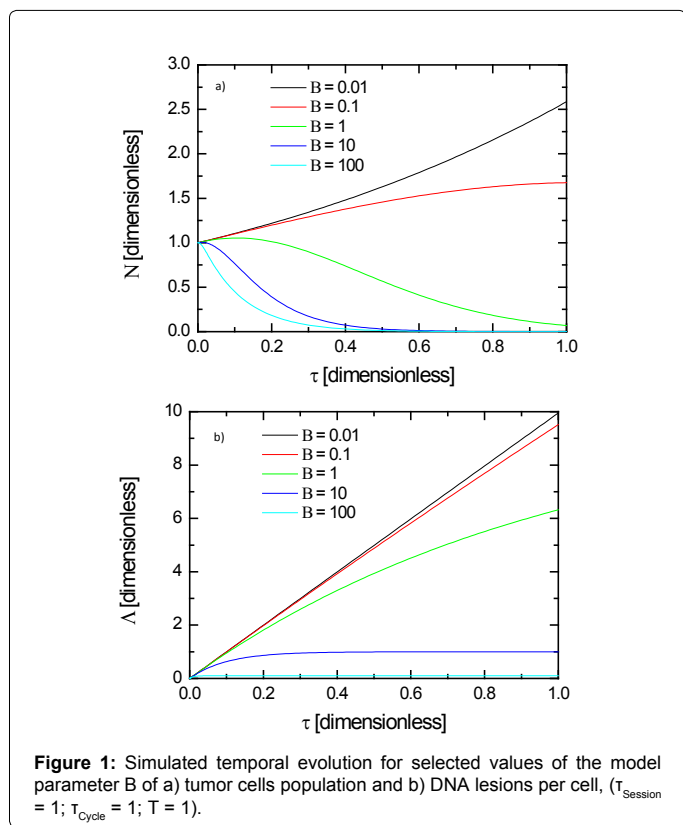
$$A^* = \frac{4DY\Sigma(1-a)\phi}{k_B n t_{\text{Session}}} \quad (33)$$

The dimensionless mathematical model presented in this section was solved by means of the commercial software COMSOL Reaction Engineering Lab 1.4[®]. Absolute and relative tolerances adopted in the calculation were both equal to $1 \cdot 10^{-10}$, whereas initial and maximum steps were set to $1 \cdot 10^{-9}$ and 0.01, respectively.

Model Results and Discussion

Numerical results of the dimensionless model presented in the previous section are illustrated in the following. The initiation of radiotherapy was set by $\tau=0$, while $N=1$ represents the population of clonogenic tumor cells at the beginning of the treatment. For an initial investigation, the exponential growth kinetics was selected while the following set of values was given to the model parameters: $A^*=10$; $X=0$; $\Delta=0$; $\tau_{\text{Session}}=1$; $\tau_{\text{Cycle}}=1$; $T=1$. On the other hand, the parameter B was varied in the range 0.01-100. Recalling Equation 22, it is worth repeating that high values of B indicate faster DNA damages fixation with respect to cells proliferation. Conversely, low B values mean that tumor cells repopulation has a higher rate than the one of DNA lesions linear repair mechanism.

Figure 1a displays the time (dimensionless) evolution of the tumor cell population for selected values of the parameter B. It can be seen that when $B=0.01$ the number of tumor cells keeps increasing even if radiation is delivered ($A^*=10$) to the population. When the parameter B is equal to 0.1, the tumor cell population grows with a rate that decreases as the treatment time is prolonged up to $\tau=T$. A different behavior can be obtained when B is set to 1. The number (dimensionless) of tumor cells increases up to reach a maximum at τ equal to about 0.1. Then, cell population starts to shrink as a consequence of the higher number of cells killed by DNA damages with respect to the number of new cells formed by proliferation. However, it can be observed that the number of tumor cells at the end of the radiation treatment, i.e., $\tau=T$, is still significant. This means that the radiation dose delivered (taken into account by the parameter A) does not result in an effective treatment if the values of B (which can be understood as the biophysical characteristics of the tumor) is less than or equal to one. On the other hand, the same treatment can be effective for tumor populations whose biophysical characteristics give higher values of the parameter B. More specifically, when B is equal to or higher than 10, it can be seen in Figure 1a that the number of tumor cells decreases to negligible levels during the course of the radiotherapy. It should be pointed out that in this work an effective radiation treatment is defined as the one that ends up with $N \leq 0.001 N_0$, while the reverse defines an unsuccessful



treatment. Although this choice may appear arbitrary, other possible definitions may be adopted without any change in the structure of the proposed model.

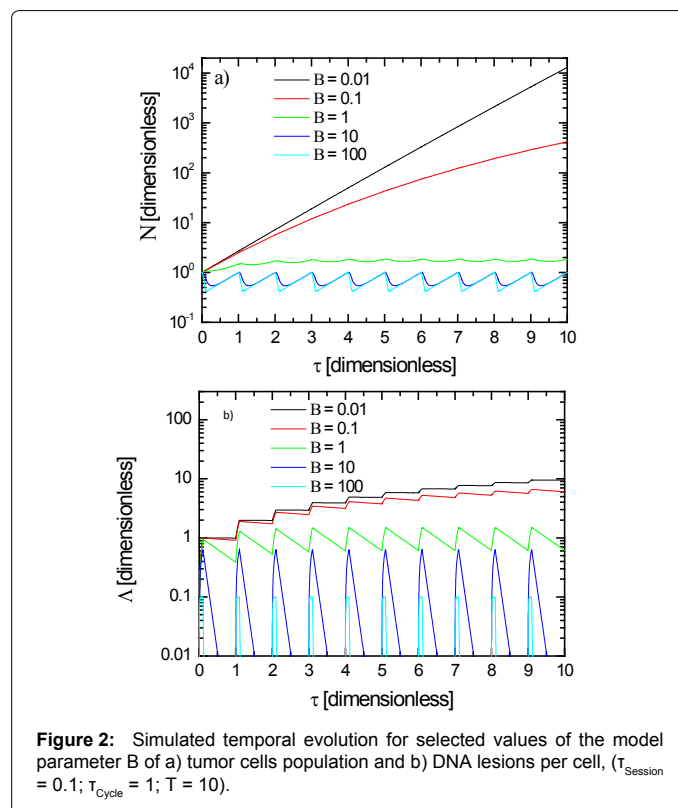
The corresponding dimensionless number of DNA lesions per cell as a function of the dimensionless time generated during the radiation treatments is shown in Figure 1b. It may be firstly seen that the number of lesions per cell decreases as B is augmented. In addition, Figure 1b clearly shows that Λ steadily increases as function of time for $B \leq 1$ while the number of lethal lesions per cell reaches a stationary value when B is greater than 10. In order to explain this behavior it can be useful to recall the two opposing phenomena that determine the number of lesions per cell. More specifically, radiation delivery produces DSBs that tumor cells attempt to repair by different mechanisms [26]. As expressed by Equation 22, higher values of the parameter B imply high rate of the repair mechanisms that, in turn, result in lower number of lesion per cells. In addition, as B increases the lesions repair rate can equate their production rate represented by the parameter A in Equation 19, which lead to the stationary values of Λ shown in Figure 1b.

By comparing Figures 1a and 1b, it can appear quite puzzling that when the radiation treatment results more effective the number of lesions per cell is lower. With the aim to clarify this finding, it is worth mentioning that the TLK model does not consider the possibility that a fatal lesion can be directly produced by the ionizing radiation [26]. Indeed, a lethal lesion, i.e., a lesion resulting in cell killing, is a consequence of attempts by the cell to fix or repair the DSBs produced by radiation exposure. Therefore, an increase of the parameter B acts in two different directions. At one hand, it increases the relative rate at which the lesions are repaired thus reducing their number per cell

(Figure 1b). On the other hand, an increase of the repair mechanisms rate increases the chances of misrepair, i.e., the number of lethal lesions produced per unit of time because of uncorrected fixation, which, in turn, increase the cell killing (Figure 1a).

The effect of parameter B was also investigated by varying the modality to administer the same dimensionless total dose ($A^*=10$) of the previous case. In particular, the following radiation administer parameters were adopted: $\tau_{\text{Session}}=0.1$; $\tau_{\text{Cycle}}=1$; $T=10$. Parameters X and Δ were set equal to zero also in this case. Figure 2a shows the results obtained by varying B in the range 0.01–100. A semi-log plot is adopted in order to highlight the different behavior of the system as B varies. The two lower values of B give an increase of the tumor cell population during the radiation treatment. This is due to low rate of DSBs repair with respect to the proliferation rate, which signifies a low production of fatal lesions. As B is increased to 1, the tumor cell population approaches a steady state because of the balance between the cell birth rate and the cell killing rate due to radiation exposure. An oscillatory behavior appears when B is set equal to 10. In this case, the dimensionless number of tumor cells oscillates around an average steady state value. This behavior is due to the decrease of tumor cells number during irradiation periods, followed by an increase during recovery time. Further increase of B does not significantly affect the average number of malignant cells, even if a more abrupt decrease of N may be observed during the irradiation periods.

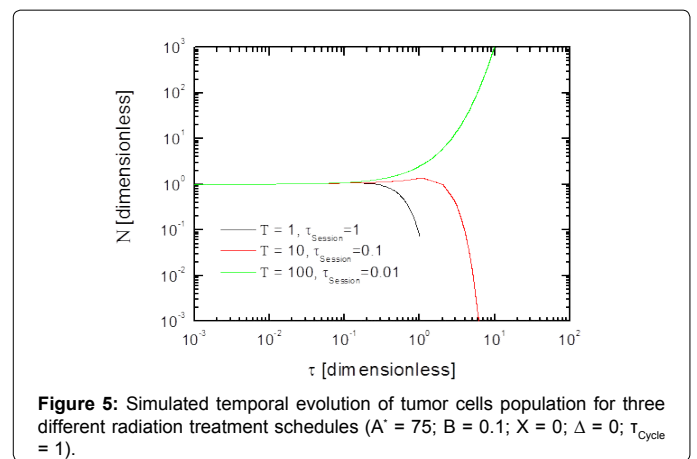
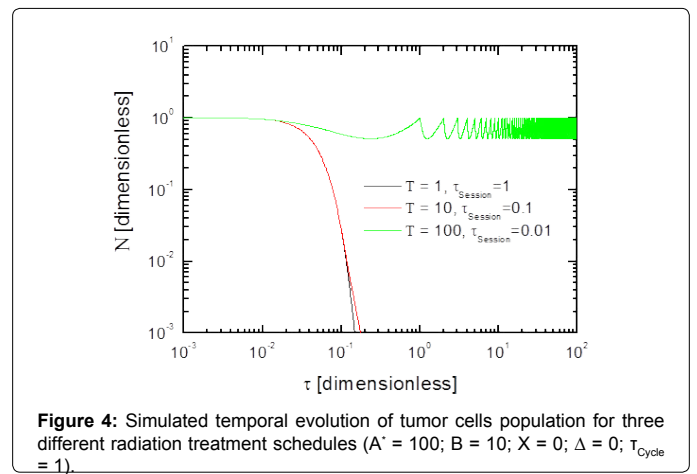
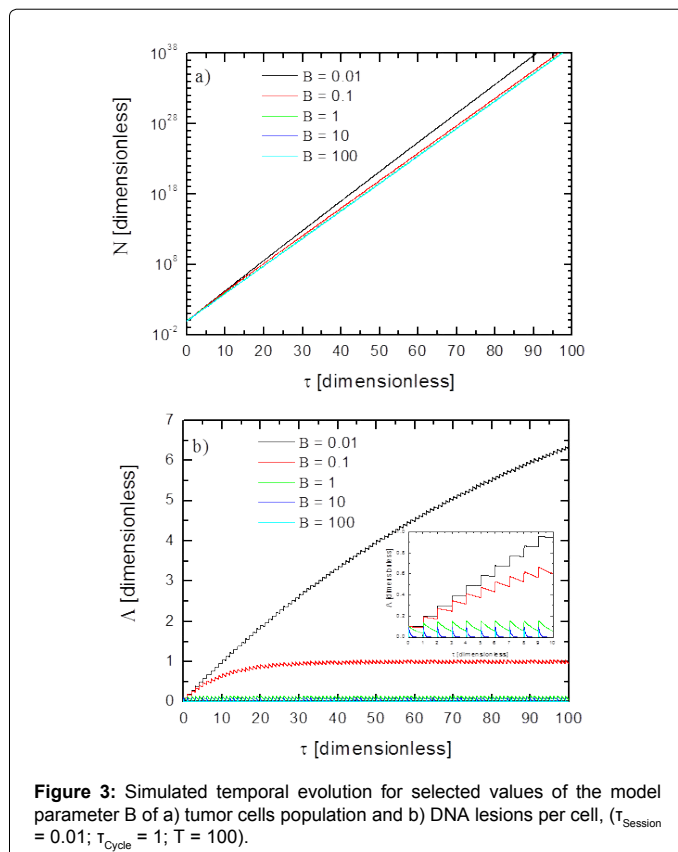
The time evolution of dimensionless number of lesion per cell corresponding to the tumor population temporal profiles shown in Figure 2a is plotted in Figure 2b. It can be seen that Λ oscillates for each of the selected values of B. This behavior arises from the fact that radiation is supplied during only one tenth ($\tau_{\text{Session}}=0.1$) of the total cycle time ($\tau_{\text{Cycle}}=1$). This means that during the first part of the cycle, lesions are produced and repaired, thus determining an increase of Λ .



Conversely, Λ decreases during the second part of the cycle since only fixation of residual lesions takes place. Moreover, it may be observed that the higher is the value of B , the stronger is the effect of the repair mechanism on the global dynamic of DNA lesions. These findings may be also related to the oscillatory behavior of N shown in Figure 2a. An increase in the number of lesion per cells also increases the fatal lesions generated by repair mechanisms, which, in turn, increases cells death rate. On the other hand, the subsequent decrease of Λ occurring during the recovery time makes the repopulation phenomenon predominant. However, it should be noted that for low values of B the tumor growth rate is too fast to be affected by radiation, which can explain the occurrence of oscillation in tumor population only for high values of B . Regarding the effectiveness of the treatment, Figure 2a reveals that none of the investigated values of B results in the tumor eradication.

Similar findings in terms of treatment effectiveness are obtained by setting the radiation exposure parameters as follows: $\tau_{\text{Session}}=0.01$; $\tau_{\text{Cycle}}=1$; $T=100$, i.e., when the dimensionless total dose is further fractionated. In particular, Figures 3a and 3b show the time evolution of N and Λ , respectively, where the same values of the previous cases for the other model parameters are maintained, i.e., $A^*=10$, $X=0$; $\Delta=0$. The tumor population increases from its initial value regardless the value of B adopted in the simulation. This is because the number of lesions produced during the radiation exposure periods is too low to affect the tumor growth. Indeed, with this dose fractionation, tumor cells have much more time to grow unrestrained, thus increasing their number. An oscillatory behavior of Λ can be observed also in this case (Figure 3b).

Results reported in Figures 1-3 show that radiation administer schedule strongly influences the effectiveness of the treatment. For



instance, by setting A^* and B both equal to 10, radiotherapy results in eradication of the tumor in the case of no fractionation (Figure 1a), while a significant number of tumor cells is present at the end of the treatment when the total prescribed dose is fractionated (Figures 2a and 3a). However, results of a series of numerical simulations performed to investigate the effect of fractionation by varying both parameters A^* and B proved that this finding could not be generalized. More specifically, the simulated time evolutions of the tumor population obtained by setting $A^*=100$, $B=10$; $X=0$; $\Delta=0$ for three different dose delivering schedules are reported in Figure 4. It can be seen that an effective treatment is attained in the case of $\tau_{\text{Session}}=1$; $\tau_{\text{Cycle}}=1$; $T=1$ and $\tau_{\text{Session}}=0.1$; $\tau_{\text{Cycle}}=1$; $T=10$. On the other hand, radiotherapy did not result in tumor eradication when the total dose was imposed according to the schedule specified by the following parameters $\tau_{\text{Session}}=0.01$; $\tau_{\text{Cycle}}=1$; $T=100$. In fact, it can be seen in the latter case that N shows an oscillating behavior around an average stationary value greater than one.

A different outcome was obtained by setting the following model parameters set $A^*=75$; $B=0.1$; $X=0$; $\Delta=0$. The dimensionless number of tumor cells is plotted in Figure 5 for the three investigated radiation exposures. It may be seen that an effective treatment was obtained by simulating the radiation delivering according the parameter $\tau_{\text{Session}}=0.1$; $T=10$. On the other hand, tumor cells are still present when a not fractionated scheme ($\tau_{\text{Session}}=1$; $T=1$) is applied or in the case of dose fractionation whose parameter $\tau_{\text{Session}}=0.01$; $T=100$. However, simulations of higher fractionation schedule show success in tumor eradication for the case of $A^*=8500$; $B=0.0003$; $X=0$; $\Delta=0$ as shown in

Figure 6, where, conversely, the inefficiency of no fractionated and low fractionated schemes is also proved by the corresponding time profiles of tumor cells population. It may also notice in Figure 6 that in the case of successful outcome a remarkable maximum of tumor cells number was reached during the treatment.

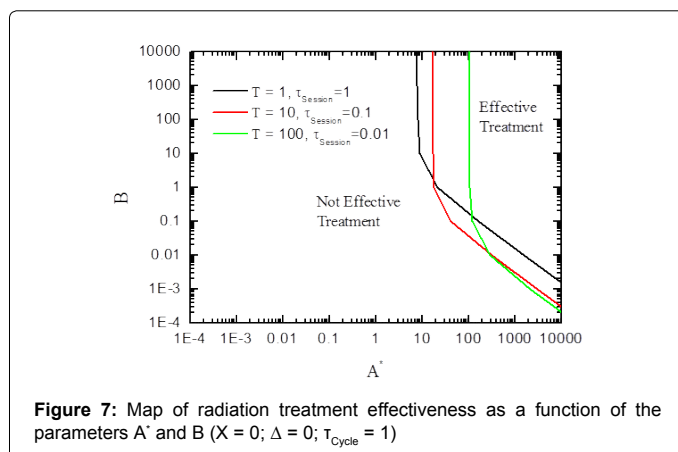
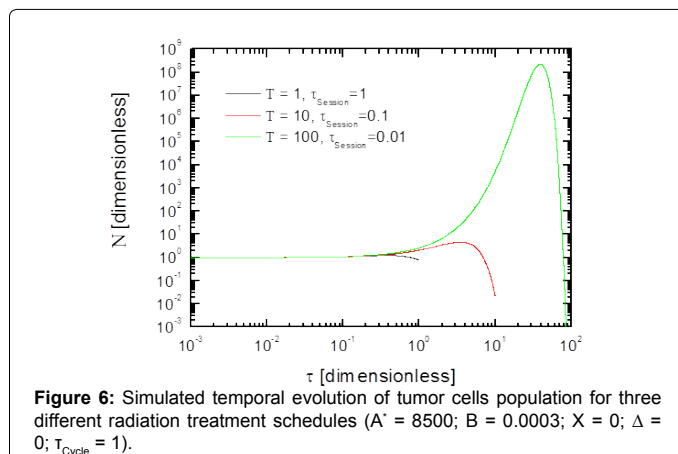
The results reported above clearly show that dose fractionation can result in successful treatment or not depending on the value of the parameters A^* and B . Or, in other words, given A^* and B values, the success of the radiation cure may depend on the treatment schedule adopted. With the aim to obtain deeper insights on this behavior, a series of numerical simulations were performed by systematically varying A^* and B , as well as the treatment schedule. The exponential kinetics was considered, while the other model parameters X and Δ were set both equal to zero. The results of these simulations are summarized in Figure 7 where a two-dimensional domain whose coordinates are the model parameters A^* and B is shown. This domain is divided in two regions by a curve for each of the investigated radiation delivery modes. On the right-hand-side of each curve the region of effective treatments extends. Conversely, the points representing the A^* - B pairs, whose values do not result in eradication of the tumor, belongs to the not effective treatments regions extending on the left-hand-side of each curve. The curves reported in Figure 7 are the loci of A^* - B pairs that lead to a tumor population N at the end of the treatment equal to 0.001. It is worth recalling that the latter condition was used in this work to define an effective radiation treatment.

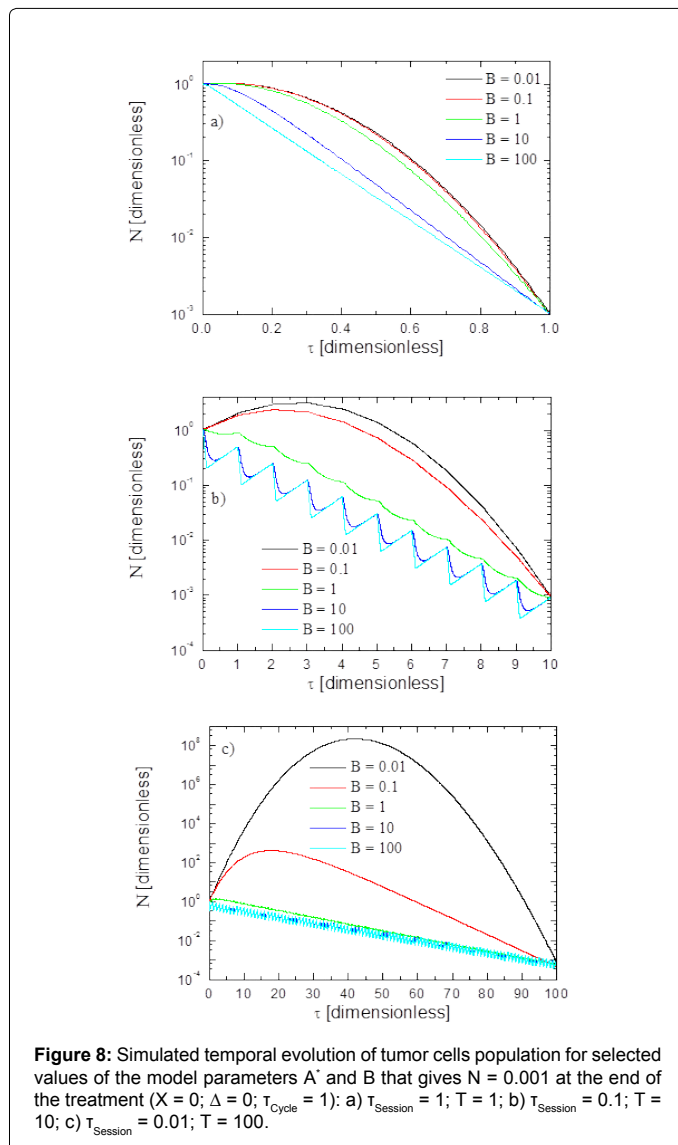
Some considerations can be gained from the analysis of Figure 7. Firstly, it can be observed that for low values of B (say smaller than

one) the value of the parameter A^* needed to attain effective treatments decreases as B increases. On the other hand, the transition between effective and not effective treatment regions tend to occur at the same value of A^* as B becomes higher than 1. This pattern can be observed regardless the fractionation scheme of the radiation exposure. These outcomes can be also examined recalling Equations 21 and 22. More specifically, the dimensionless DNA lesions production rate A^* (which quantify the effect of the radiation dose rate) required to eradicate the tumor cells decreases as the lesions repair rate increases up to the same order of magnitude of the proliferation rate ($B=1$). When the repair rate is higher than the growth rate, ($B > 1$), the DSB production rate will result in the same effect in spite of the rate of lesions repair mechanism. These findings can be explained as follows. Higher values of B means higher DSB repair rate, which, in turn, gives rise to a higher formation rate of lethal DNA damages. This fact reflects on a lower lesion production rate (quantified by the parameter A^*) required to be the radiation effective in tumor cell killing. On the other hand, higher values of A^* are needed when the lethal lesion production rate is lower due to the lower rate of repair mechanisms.

A different behavior of the system in the cases of high and low values of B can be examined also with regard to the adopted treatment schedule. Figure 7 shows that simulated radiation treatments with higher values of B will result less successful as the dose fractionation is increased. This can be appreciated focusing at the shrinking of the effective treatment region as T and τ_{Session} increases and decreases, respectively. An opposite effect can be observed for the lower investigated values of B . Indeed, the transition curve shifts to the left as the dose fractionation increases. This implies that the same total dose (Equation 21) will result more effective when it is delivered fractionated. Such a behavior can be explained as follows. By keeping constant the total radiation dose, in the case of fractionation, high values of B imply that lesions are repaired very soon after the end of the irradiation periods (cf. Figures 2b and 3b). Thus, cell killing does not take place during the recovery time and cell growth occurs unrestrained. On the other hand, when the repair mechanism is slow, more time is needed to produce fatal lesions. This additional time can be provided by increasing the fractionation, which, in turn, leads to a more effective treatment.

It may be a point of interest to analyze the dynamics of tumor cells population during successful irradiation schedules as the dimensionless repair rate B varies. Figure 8 shows numerical simulated evolutions of N as a function of dimensionless time for the three investigated treatment schedules. These results are related to A^* - B model parameters pairs whose values identify points on the corresponding transition curves reported in Figure 7. Indeed, it can be seen in Figure 8a ($\tau_{\text{Session}}=1$; $T=1$) that all the simulated treatments lead to the eradication of the tumor, i.e., $N=0.001$ at $\tau=T$. However, the rate of cells decreasing is different for the diverse values of B . Specifically, in the case of higher values of B the tumor population decreases faster during the first part of the treatment. Conversely, when B is low, N slightly increases at the beginning of the treatment up to reach a maximum. Then, a decrease of the tumor cells number is observed up to the end of the treatment. The response of the system in the case of fractionated radiation dose ($\tau_{\text{Session}}=0.1$; $T=10$) is shown in Figure 8b. It may be observed that tumor population reaches a maximum during the treatment, being the number of cells corresponding to this maximum higher with respect to the one observed in case shown in Figure 8a. It may be also seen that this maximum increases its value as B decreases, up to achieve a tumor population of the order of about three times the initial population for very low values of B . On the other hand, the tumor cells population decreases monotonically for higher values of B , even if an oscillatory

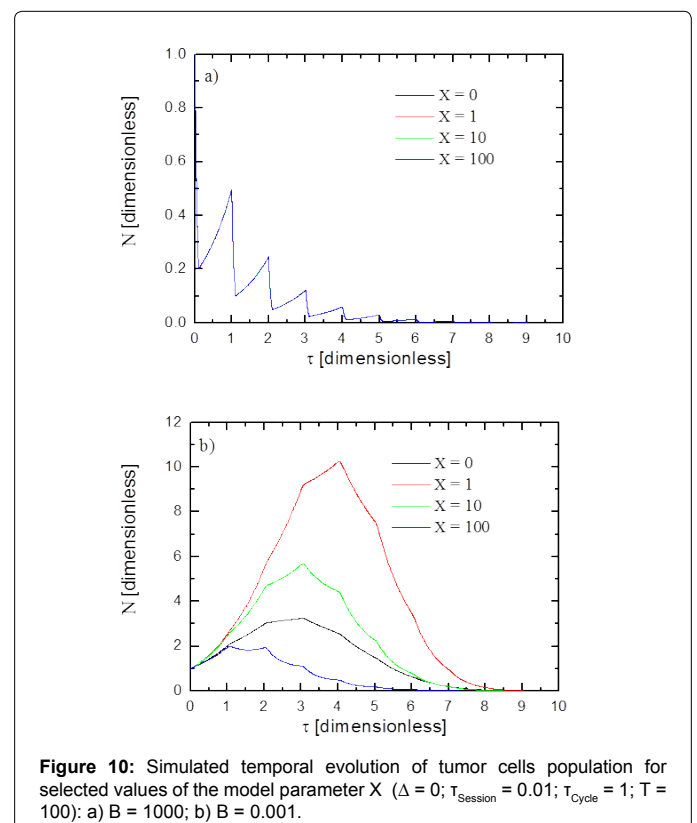
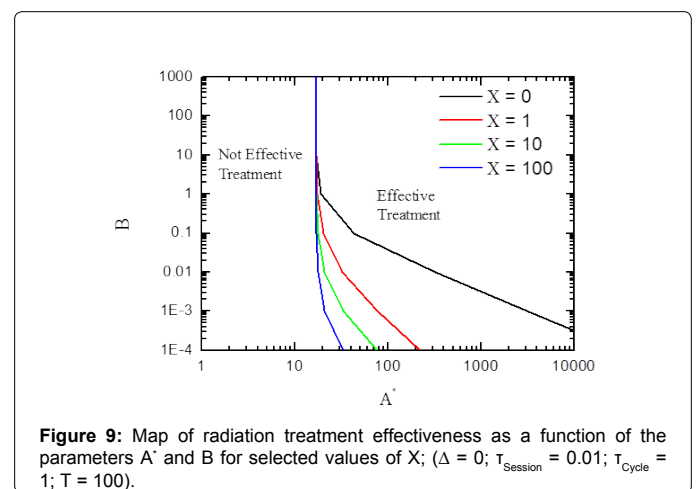




behavior due to the alternation of irradiation and recovery periods can be seen. The different evolution of the system for high or low values of the parameter B is a consequence of the repopulation phenomena occurring during the treatment. Indeed, higher values of B make lethal lesions quickly produced, thus leading to rapid cell killing. In contrast, lower value of B means a slower formation of fatal lesions in cell DNA. This creates the opportunity for clonogenic cells to reproduce making the population increases in number. Then, as might be expected, once the number of lethal DSBs reaches a proper level, cell killing becomes dominant thus decreasing the tumor cell population up to eradicate it. A similar response of the system is obtained when the same total radiation dose is further fractionated ($\tau_{\text{Session}} = 0.01$; $T = 100$). However, a more remarkable increase in tumor cells number during the treatment and a more pronounced oscillatory behavior can be observed for lower and higher values of B , respectively.

The effect of the parameter X on the effectiveness of the simulated radiation treatment is illustrated in Figure 9. The latter was obtained by means of the same procedure Figure 7 was derived by. The investigated kinetics is the exponential one, whereas the other model parameters

were set as $\Delta = 1$; $\tau_{\text{Session}} = 0.01$; $\tau_{\text{Cycle}} = 1$; $T = 100$. It can be clearly seen that an increase of X shifts the transition curve to the left, which, in turn, make the effective treatment region broader. This finding can be explained recalling that an increase of X implies an increasing importance of the damages misrepair mechanisms Equation 26. In other words, by augmenting X more lethal lesions are produced due to the additional contribution of the quadratic terms appearing in Equation 21. However, it clearly appears in Figure 9 that this effect vanishes as at higher values of the dimensionless linear repair rate B increases. Indeed, in this case the repopulation rate of tumor cells is slow enough to make the lethal lesions produced by the linear mechanism only sufficient to eradicate the tumor. On the other hand, lower values of B imply higher tumor growth rates. Under these



conditions the additional fatal lesions produced by misrepair help to increase the tumor cells killing by radiation.

Further tests of the model radiation response to variations of the parameter X were carried out comparing the time evolution of the tumor cells population. Figure 10a shows the effect of X variation when $B=1000$. The values of A^* are those corresponding to the A^*-B coordinate pairs of the transitions curves appearing in Figure 9. It may be seen that variation of X does not significantly influence the time evolution of the tumor population. A different behavior is observed in Figure 10b where the results related to the case of $B=0.001$ are reported. All simulations show an increase of the cell population at the beginning of the treatment followed by a decrease down to the level that identify the eradication of the tumor ($N=0.001$ at $\tau=T$). However, the maximum number of tumor cells reached during the treatment strongly depends on the values of X . In particular, it can be seen that the maximum value of N increases as X is increased from zero to 1. Then, a reduction of the maximum number of tumor cells during the treatment is observed when X is increased to 10 and 100. Also this non monotonic outcome of the parameter X can be ascribed to the opposite effect of repair mechanisms in the framework of the TLK model. Indeed, on one hand, an increase of the rate of repair reduces the number of DNA lesions in tumor cells thus making them clonogenic. The system response will result in a higher number of tumor cells. On the other hand, fast repair mechanisms can also augment the chance of misrepair, i.e., formation of lethal lesions, thus increasing the cell killing and consequently reducing the cell population.

The results of simulating radiotherapy treatments by varying the parameter Δ are reported in Figure 11. It may be clearly seen the effective treatment region increasing as this model parameter increases. This finding can be grasped on the base of the defining equation of Δ (Equation 27). Indeed, it represents the ratio between the probabilities of binary and linear repair mechanisms not to result in correct fixation, thus leading to lethal lesions formation and cells killing. Therefore, the rate of the latter phenomenon increases as Δ becomes larger.

So far it has been simulated radiotherapy treatments during which tumor cells proliferate according to the exponential kinetics. In order to make a comparison between the latter and the logistic and Gompertz kinetics, another series of numerical simulation were carried out. Related results are summarized in Figure 12, which was constructed according to the same method adopted in the case of Figures 7, 9 and 11. It can be noticed that transition curves of exponential and logistic kinetics are very similar. Vice versa, a different partition of the A^*-B

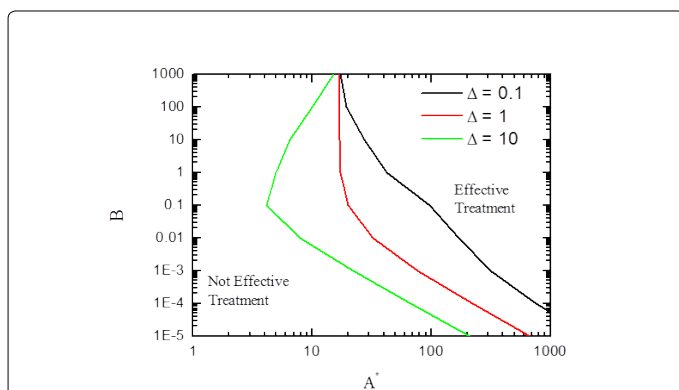


Figure 11: Map of radiation treatment effectiveness as a function of the parameters A^* and B for selected values of Δ ($X = 1$; $\tau_{\text{Session}} = 0.1$; $\tau_{\text{Cycle}} = 1$; $T = 10$).

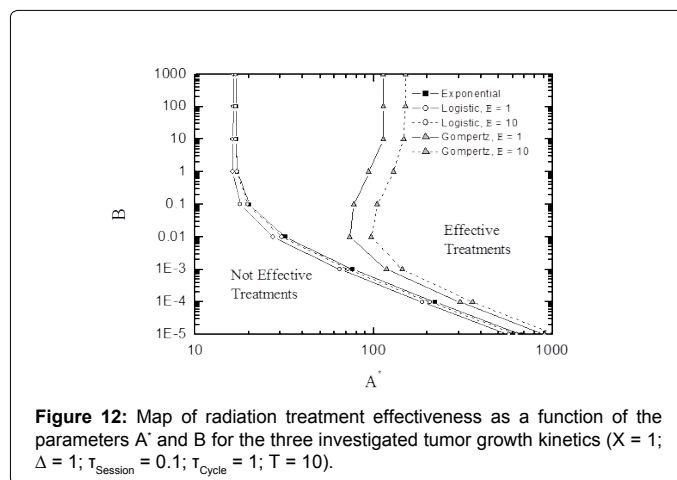


Figure 12: Map of radiation treatment effectiveness as a function of the parameters A^* and B for the three investigated tumor growth kinetics ($X = 1$; $\Delta = 1$; $\tau_{\text{Session}} = 0.1$; $\tau_{\text{Cycle}} = 1$; $T = 10$).

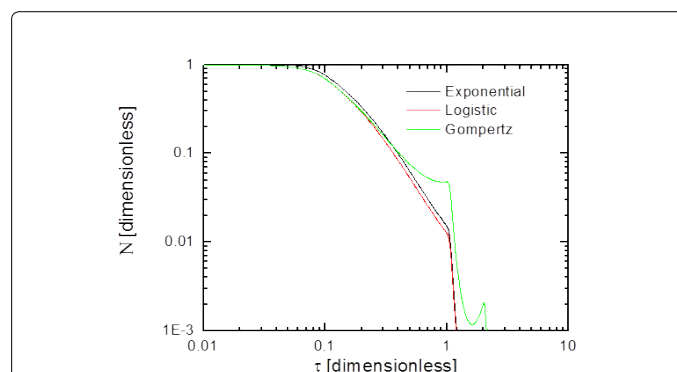


Figure 13: Simulated temporal evolution of tumor cells population for the three investigated kinetics ($A^* = 100$, $B = 0.1$; $X = 1$; $\Delta = 1$; $\tau_{\text{Session}} = 0.1$; $\tau_{\text{Cycle}} = 1$; $T = 10$).

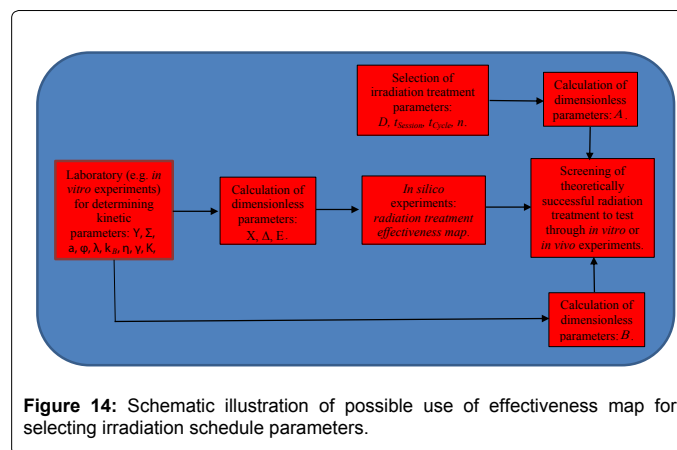


Figure 14: Schematic illustration of possible use of effectiveness map for selecting irradiation schedule parameters.

model parameter domain can be observed in the case of Gompertz kinetics. Specifically, the associated effective treatment region extends less than the other investigated kinetics. It can be also seen that this difference becomes larger as B increases. In addition, Figure 12 shows that the effect of the parameter E is more marked in the case of the Gompertz law with respect to the logistic one. Additional insights of this different behavior can be gained by Figure 13 where the evolution of tumor cell population following the three investigated kinetics are reported. These results are related to the following set of parameters:

$A^*=100$; $B=0.1$; $X=1$; $\Delta=1$; $E=1$; $\tau_{\text{Session}}=0.1$; $\tau_{\text{Cycle}}=1$; $T=10$. It can be seen that when the number of tumor cells decreases the repopulation phenomenon occurs faster in the case of Gompertz kinetics. This will result in longer treatment time to eradicate the tumor. Findings illustrated in Figures 12 and 13 are in agreement with the ones reported by other authors who investigated the effect of various growth mechanisms by using the linear-quadratic (LQ) model to describe the radiation-tumor cells interaction [25].

Finally, it may be worth illustrating a possible use of the radiation treatment effectiveness map developed in this work. The main goal is to reduce the number of experiments needed to ascertain the optimal irradiation schedule. The basic idea is schematically represented in Figure 14. Once the specific tumor cell line of interest is selected, a series of *in vitro* experiments could be performed to determine the kinetic parameters characterizing growth and radiation-induced death of tumor cells. Then, dimensionless parameters can be calculated and a series of numerical simulations (*in silico* experiments) is implemented to achieve the effectiveness map. This way, representative points of possible irradiation schedules may be mapped out through preceding calculation of the corresponding A and B coordinates. Thus, at least in principle, this procedure leads to a selection of theoretically successful treatments to validate experimentally.

Concluding Remarks

The aim of this work was to develop a mechanistic model able to describe radiation damages on tumor cells when repopulation occurs simultaneously to DNA lesions repair. Whilst the proposed model is clearly a gross oversimplification of a highly complex multiscale biological system, some information about the effect of repopulation during radiotherapy can be gained.

A fundamental role is played by ratio between the rate of DNA lesions repair mechanisms and tumor growth rate, i.e., the dimensionless parameter B defined in this work. Specifically, it was found that an increase in the fractionation of the total radiation dose to be administered results in a less effective treatment for high values of B. Vice versa, for low values of B better results in terms of tumor eradication were obtained by increasing the total prescribed dose fractionation. Calculations based on the present analysis also indicate that significant variations in tumor population dynamics and radiation treatment effectiveness emerge depending on the form of the cells growth kinetics. Exponential and logistic growth laws produce similar results but the Gompertz kinetics was shown to result in significantly less tumor eradication. Moreover, the higher the repair rate of cell line with respect to its growth rate, the greater the difference in treatment outcomes

It is hoped that this model will provide a useful tool for further investigation in the context of external beam radiotherapy. Comparison with experimental data reported in the literature is already along the way. Future directions of this study would be also the incorporation of the other "Rs" of radiotherapy, i.e., reoxygenation, redistribution, and resensitization in the framework of the TLK model.

Nomenclature

a	correctness coefficient of linear misrepair mechanisms, - ;
B	birth rate, h^{-1} ;
D	total dose, Gy;
\dot{D}	dose rate, $Gy h^{-1}$;

H	radiation-induced death rate, h^{-1} ;
h	hazard rate, h^{-1} ;
K	cell carrying capacity, - ;
k_B	kinetic constant, h^{-1} ;
\bar{L}	number of DSBs per cell, - ;
N	number of tumor cells, - ;
n	number of cycles, - ;
S	survival probability, - ;
T	treatment time, h ;
t	time, h ;
t_{Cycle}	cycle time, h ;
t_{Session}	irradiation time, h ;
Y	DSB yield, Gy^{-1} ;

Greek letters

A	dimensionless group defined by Eq. (24);
A^*	dimensionless group defined by Eq. (33);
B	dimensionless group defined by Eq. (25);
X	dimensionless group defined by Eq. (26);
Δ	dimensionless group defined by Eq. (27);
E	dimensionless group defined by Eq. (28);
φ	partition coefficient of simple (type 1) DSBs, - ;
γ	partition coefficient complex (type 2) DSBs, - ;
Λ	dimensionless number of lesion per cell, - ;
N	dimensionless number tumor cell, - ;
λ	linear repair kinetic constant, h^{-1} ;
η	binary misrepair kinetic constant, h^{-1} ;
Σ	DSB formation probability, - ;
τ	dimensionless time, - ;

Subscripts

0	initial;
1	simple (type 1) DSBs;
2	complex (type 2) DSBs;
f	lethal;
r	reference value;
s	scaling value;

References

- Oldham M (2001) Radiation physics and applications in therapeutic medicine. Physics Education 36: 460-467.
- Enderling H, Chaplain MA, Hahnfeldt P (2010) Quantitative modeling of tumor dynamics and radiotherapy. Acta Biotheor 58: 341-353.
- Thames HD, Hendry JH (1987) Fractionation in radiotherapy. Taylor and Francis, London.

4. Brenner DJ, Hlatky LR, Hahnfeldt PJ, Hall EJ, Sachs RK (1995) A convenient extension of the linear-quadratic model to include redistribution and reoxygenation. *International Journal of Radiation Oncology Biology Physics* 32: 379-390.
5. Withers HR, Taylor JM, Maciejewski B (1988) The hazard of accelerated tumor clonogen repopulation during radiotherapy. *Acta Oncol* 27: 131-146.
6. Sachs RK, Heidenreich WF, Brenner DJ (1996) Dose timing in tumor radiotherapy: considerations of cell number stochasticity. *Math Biosci* 138: 131-146.
7. Yakovlev AY, Zorin AV (1988) *Computer simulation in cell radiobiology*. Springer-Verlag, Berlin.
8. Jones B, Dale RG (2007) Further radiobiologic modeling of palliative radiotherapy: use of virtual trials. *Int J Radiat Oncol Biol Phys* 69: 221-229.
9. Withers HR (1975) The four r's of radiotherapy. *Advances in Radiation Biology* 5:241-247.
10. Steel GG, McMillan TJ, Peacock JH (1989) The 5Rs of radiobiology. *Int J Radiat Biol* 56: 1045-1048.
11. O'Rourke SF, McAneney H, Hillen T (2009) Linear quadratic and tumour control probability modelling in external beam radiotherapy. *J Math Biol* 58: 799-817.
12. Wheldon TE, Kirk J, Orr JS (1977) Optimal radiotherapy of tumour cells following exponential-quadratic survival curves and exponential repopulation kinetics. *Br J Radiol* 50: 681-682.
13. Fowler JF (1989) The linear-quadratic formula and progress in fractionated radiotherapy. *Br J Radiol* 62: 679-694.
14. Saunders MI, Dische S, Barrett A, Parmar MK, Harvey A, et al. (1996) Randomised multicentre trials of CHART vs conventional radiotherapy in head and neck and non-small-cell lung cancer: an interim report. CHART Steering Committee. *Br J Cancer* 73: 1455-1462.
15. Fowler JF (2001) Biological factors influencing optimum fractionation in radiation therapy. *Acta Oncol* 40: 712-717.
16. O'Donoghue JA (1997) The response of tumours with Gompertzian growth characteristics to fractionated radiotherapy. *Int J Radiat Biol* 72: 325-339.
17. Wheldon EG, Lindsay KA, Wheldon TE (2000) The dose-response relationship for cancer incidence in a two-stage carcinogenesis model incorporating cellular repopulation. *International Journal of Radiation Biology* 76: 699-710.
18. Lindsay KA, Wheldon EG, Deehan C, Wheldon TE (2001) Radiation carcinogenesis modeling for risk of treatment-related second tumours following radiotherapy. *British Journal of Radiology* 74: 529-536.
19. Mao JH, Lindsay KA, Mairs RJ, Wheldon TE (2001) The effect of tissue-specific growth patterns of target stem cells on the spectrum of tumours resulting from multistage tumorigenesis. *J Theor Biol* 210: 93-100.
20. McAneney H, O'Rourke SF (2007) Investigation of various growth mechanisms of solid tumour growth within the linear-quadratic model for radiotherapy. *Phys Med Biol* 52: 1039-1054.
21. Badoual M, Gerin C, Deroulers C, Grammaticos B, Llitjos JF, et al. (2014) Oedema-based model for diffuse low-grade gliomas: application to clinical cases under radiotherapy. *Cell Prolif* 47: 369-380.
22. Unkelbach J, Craft D, Hong T, Papp D, Ramakrishnan J, et al. (2014) Exploiting tumor shrinkage through temporal optimization of radiotherapy. *Phys Med Biol* 59: 3059-3079.
23. Voyant C, Julian D, Roustit R, Biffi K, Lantieri C (2013) Biological effects and equivalent doses in radiotherapy: A software solution. *Rep Pract Oncol Radiother* 19: 47-55.
24. Nawrocki S, Zubik-Koval B (2015) Clinical Study and numerical simulation of brain cancer dynamics under radiotherapy. *Communications in Nonlinear Science and Numerical Simulation* 22: 564-573.
25. Rockne RC, Trister AD, Jacobs J, Hawkins-Daarud AJ, Neal ML, et al. (2015) A patient-specific computation model of hypoxia-modulated radiation resistance in glioblastoma using 18F-FMIO-PET. *J R Soc Interface* 12.
26. Stewart RD (2001) Two-lesion kinetic model of double-strand break rejoining and cell killing. *Radiat Res* 156: 365-378.
27. Krantz WB (2007) *Scaling analysis in modeling transport and reaction processes*. John Wiley Sons Inc Hoboken, New Jersey.
28. Michelson S, Leith JT (1993) Growth factors and growth control of heterogeneous cell populations. *Bull Math Biol* 55: 993-1011.
29. Sachs RK, Hlatky LR, Hahnfeldt P (2001) Simple ODE models of tumor growth and anti-angiogenic or radiation treatment. *Mathematical and Computer Modelling* 33:1297-1305.
30. Sachs RK, Hahnfeldt P, Brenner DJ (1997) The link between low-LET dose-response relations and the underlying kinetics of damage production/repair/misrepair. *International Journal of Radiation Biology* 72: 351-374.
31. Guerrero M, Stewart RD, Wang JZ, Li XA (2002) Equivalence of the linear-quadratic and two-lesion kinetic models. *Phys Med Biol* 47: 3197-3209.